Heliyon 10 (2024) e23832

Contents lists available at ScienceDirect

Heliyon

journal homepage: www.cell.com/heliyon

Vitamin D receptor induces oxidative stress to promote esophageal squamous cell carcinoma proliferation via the p53 signaling pathway☆

Qi-Xin Shang [a,1], Yu-Shang Yang [a], Han-Lu Zhang [a], Ya-Ping Cheng [b], Han Lu [b], Yong Yuan [a], Long-Qi Chen [a,**], Ai-Fang Ji [b,*,1]

[a] Department of Thoracic Surgery, West China Hospital of Sichuan University, Chengdu, Sichuan, China
[b] Heping Hospital Affiliated to Changzhi Medical University, No. 161 Jiefang East Street, Changzhi, 046000, China

ARTICLE INFO

Keywords:
Esophageal squamous cell carcinoma
VDR
Cell phenotype
TMT proteomics
p53 signaling pathway
Oxidative stress
Tumor formation in nude mice

ABSTRACT

Background: Esophageal squamous cell carcinoma (ESCC) is a common pathological esophageal cancer with poor prognosis. Vitamin D deficiency reportedly occurs in ESCC patients, and this is related to single nucleotide polymorphism of vitamin D receptor (VDR).
Objective: We investigated the effect of VDR on ESCC proliferation, invasion, and metastasis and its potential mechanism.
Methods: ESCC and normal tissues were collected from 20 ESCC patients. The ESCC tissue microarray contained 116 pairs of ESCC and normal tissues and 73 single ESCC tissues. VDR expression and its clinicopathological role were determined by real-time quantitative polymerase chain reaction, Western blot, and immunohistochemistry staining. sh-VDR and VDR overexpression were used to validate the effect of VDR on ESCC cell phenotype, and tandem mass tag-based quantitative proteomics and bioinformatics methods identified differential VDR-related proteins. The downstream pathway and regulatory effect were analyzed using ingenuity pathway analysis (IPA). Differentially expressed proteins were verified through parallel reaction monitoring and Western blot. In vivo imaging visualized subcutaneous tumor growth following tail vein injection of VDR-deficient ESCC cells.
Results: High VDR expression was observed in ESCC tissues and cells. Gender, T stage, and TNM stage were related to VDR expression, which was the independent prognostic factor related to ESCC. VDR downregulation repressed ESCC cell proliferation, invasion, and migration in vitro and subcutaneous tumor growth and lung metastases in vivo. The cell phenotype changes were reversed upon VDR upregulation, and differential proteins were mainly enriched in the p53 signaling pathway. TP53 cooperated with ABCG2, APOE, FTH1, GCLM, GPX1, HMOX1, JUN, PRDX5, and SOD2 and may activate apoptosis and inhibit oxidative stress, cell metastasis, and proliferation. TP53 was upregulated after VDR knockdown, and TP53 downregulation reversed VDR knockdown-induced cell phenotype changes.

☆ Long-Qi Chen and Ai-Fang Ji **are co-corresponding author of this study.**

* Corresponding author. Heping Hospital Affiliated to Changzhi Medical University, No. 161 Jiefang East Street, Changzhi, 046000, China.
** Corresponding author. Department of Thoracic Surgery, West China Hospital of Sichuan University, No. 37, Guoxue Alley, Chengdu, Sichuan, 610041, China.
E-mail addresses: drchenlq@scu.edu.cn (L.-Q. Chen), jiaifang2003@163.com (A.-F. Ji).
[1] Qi-Xin Shang , Yu-Shang Yang, and Han-Lu Zhang contributed equally to this work.

https://doi.org/10.1016/j.heliyon.2023.e23832
Received 16 May 2023; Received in revised form 5 December 2023; Accepted 13 December 2023
Available online 23 December 2023

Conclusions: VDR may inhibit p53 signaling pathway activation and induce ESCC proliferation, invasion, and metastasis by activating oxidative stress.

1. Introduction

Esophageal cancer is the sixth most malignant cancer worldwide, with 456,000 new cases and 400,000 deaths annually [1,2]. At present, esophageal squamous cell carcinoma (ESCC) is the most common type of esophageal cancer in China, accounting for 90 % of esophageal cancer cases [2]. Furthermore, research on its pathogenesis and related risk factors is still ongoing. In developing countries, dietary factors are a key cause of esophageal cancer, for which dietary imbalance is the main risk factor [2]. Dietary imbalance mainly manifests as uneven and insufficient nutrient intake, and dietary nutrients are also closely related to tumorigenesis of gastrointestinal tumors [2]. Many biologically active chemicals in the diet can activate or inhibit certain genes to promote the pathogenesis of cancer [3]. In our previous study, riboflavin (vitamin B group) deficiency was found in patients with ESCC, and the single nucleotide polymorphism (SNP) in the coding region of the riboflavin transporter C20orf54 gene was found to be significantly related to the genetic susceptibility of ESCC [3]. These results suggest that both genetic and environmental factors can affect tumorigenesis of esophageal cancer. Meanwhile, we also studied the nutritional level of vitamin D, which is another nutritional factor related to esophageal cancer. Furthermore, we found that there was a lack of vitamin D in patients with ESCC [3]. Study of gene mutations related to the vitamin D metabolism pathway and susceptibility to ESCC confirmed that an increase in plasma 25(OH)D levels is associated not only with a reduced risk of ESCC, but also with the occurrence of esophageal cancer and the SNP of the vitamin D receptor (VDR) [4].

VDR belongs to the transcriptional regulator family, which includes thyroid hormone receptors, steroids, retinoic acid receptors, and retinoid X receptor (RXR) [5,6]. VDR is encoded by a gene located on chromosome 12 [7], with a total of 14 exons (eight protein-coding exons are numbered II–IX, and the other six coded VDR genes are numbered IA–IF at the 5′ end) that are controlled by two promoter regions [8,9]. The expression level of VDR and its genetic variation are important determinants of vitamin D activity and function [10]. Vitamin D3 enters the cell through the plasma membrane protein and subsequently binds to VDR and RXR [11] to form a heterodimer [11–14]. According to previous studies, the VDR-RXR complex binds to specific vitamin D response elements (VDREs) in the promoter regions of genes responsible for activating or inhibiting specific cellular pathways involved in tumorigenesis [11–14]. These pathways include various processes related to the cell cycle (cell proliferation, invasion, apoptosis, differentiation, and metastasis), regulation of immune cell differentiation [15], and inhibition of angiogenesis in malignant cells [16]. These functions involve many genes, such as p21/WAF1, *c*-myc, and JUN, that are important for cell cycle regulation and tumorigenesis [17–20]. At the same time, VDR gene polymorphism and VDR-mediated signaling pathways play an important role in cancer tumorigenesis [5,21,22].

Current research on the role of VDR in cancer has mostly been conducted in the context of colon cancer [15,20], breast cancer [22], melanoma [16,17,19], and prostate cancer [21]. In esophageal cancer, more studies on the relationship between VDR and esophageal cancer have been conducted in terms of esophageal adenocarcinoma, and the expression level of VDR decreases as tumor differentiation declines [23,24]. Only Zhou et al. [25] and Bao et al. [26] have reported the relationship between VDR expression and prognosis in ESCC stromal cells, as well as the difference at the mRNA level; however, neither of these studies explored the specific role of VDR in ESCC at the molecular level. VDR reportedly plays a major role in regulating cell proliferation, differentiation, and inducing apoptosis [27], and VDR is likely to promote cancer. However, more studies have focused on researching the effect and mechanism of vitamin D-mediated tumor suppression, while few have investigated the relationship between VDR and cell function. Therefore, taking our previous results into consideration, this study aimed to explore the role of VDR in ESCC tumorigenesis and its signaling pathways.

2. Methods

2.1. Patients

A total of 20 ESCC patients who underwent radical esophagectomy at Department of Thoracic Surgery, West China Hospital of Sichuan University from December 2018 to January 2019 were included in this study. Cancer tissues and adjacent normal tissues (8–10 cm from the original tumor boundary) were collected from patients. All patients were informed of the risks of the operation. Permission to use resected specimens and written consent were obtained from the study participants preoperatively.

The exclusion criteria included patients who underwent palliative surgery or R1 and R2 resection, received neoadjuvant therapy before surgery, were pathologically diagnosed with other types of esophageal cancer preoperatively, or had metastasis that was found during the preoperative examination.

2.1.1. Follow-up

The patients in the present study were followed up every 3 months for the first and second year, every 6 months for the third to fifth year after the treatment, and finally, every year after the fifth year. Blood routine, gastroscopy, chest compute tomography (CT), neck and abdominal ultrasound were performed as necessary according to the patient's symptoms and physical examination. The tumor status (including tumor metastasis and recurrence) and the patients' status (including survive and death) were all recorded not only

through outpatient follow-up but also through telephone and mail follow-up.

2.2. The Cancer Genome Atlas (TCGA) analysis

The data sets used for analyzing VDR mRNA expression levels of esophageal cancer patients were obtained from the TCGA data portal (https://tcga-data.nci.nih.gov/tcga). The TCGA-ESCA dataset containing 11 normal esophagus and 184 ESCC samples was analyzed for VDR expression.

2.3. Immunohistochemistry staining and scoring

The ESCC tissue microarray (TMA) included 116 cases of ESCC and matched adjacent normal esophagus tissues, as well as 73 single cases of ESCC with complete clinical information provided by Shanghai Outdo Biotech Co., Ltd. (Shanghai, China). Immunohistochemical staining was performed according to a previously described method [10]. The tissue sections were first kept at 60 °C for 24 h. Xylene deparaffinization and hydration were then carried out with an ethanol gradient (100–60 %). Antigen retrieval was performed by heating sections in 10 mM citrate (pH 6.0) boiling buffer for 15 min. TMA sections were incubated overnight at 4 °C with rabbit monoclonal *anti*-VDR antibody (1:2,000, Santa Cruz Biotechnology, Santa Cruz, CA, USA). Incubation with the corresponding secondary antibody (Rabbit IgG, 1:5,000, Santa Cruz Biotechnology) was performed the next day at room temperature for 30 min, followed by staining with 3,3′-diaminobenzidine (DAB) and hematoxylin. TMA results were viewed and photographed with the Olympus BX53 fluorescence microscope (Tokyo, Japan). A composite score was determined using a previously described method [28].

2.4. RNA isolation and reverse transcription-quantitative polymerase chain reaction (RT-qPCR)

Total RNA was isolated from cell lines using the Trizol (Thermo Fisher Scientific) according to the manufacturer's protocols. Complementary DNA synthesis of mRNA was performed using *M*-MLV reverse transcriptase (Promega Corporation, Fitchburg, WI, USA). VDR mRNA expression levels were evaluated using PCR with an SYBR green PCR master mix (Thermo Fisher Scientific) and calculated using the $2^{-\Delta\Delta Cq}$ method via normalization to GAPDH. The thermocycling conditions were as follows: 95 °C for 10 min, 45 cycles of 95 °C for 15 s, and 60 °C for 1 min. All reactions were performed in triplicate, and the primer sequences are as follows (5′–3′): VDR, forward: GCTAAGATGATACCAGGATTCAG, reverse: ATGATGACCTCAATGGCACTT; and GAPDH, forward: TGACTTCAACAGCGACACCCA, reverse: CACCCTGTTGCTGTAGCCAAA.

2.5. Western blotting

After washing with cold phosphate-buffered saline (PBS) and pelleting, the protein concentration was determined using a bicinchoninic acid assay. After electrophoresis on SDS-PAGE, proteins were transferred onto PVDF membranes. The membranes were blocked with 5 % nonfat milk and incubated with primary antibodies at 4 °C overnight. The corresponding horseradish peroxidase (HRP)-conjugated secondary antibody was added and incubated at room temperature for 2 h. Signals were visualized using an enhanced chemiluminescence reaction with an HRP substrate. The primary antibodies against VDR, TP53, APOE SOD2, and JUN were purchased from Cell Signaling Technology (Beverly, MA, USA). The antibody against β-actin was purchased from Sigma-Aldrich Co. (St Louis, MO, USA). The antibody information is listed in Table 1 in supplementary.

2.6. Cell lines and cell culture

Het-1a, KYSE-30, KYSE-410, TE-1, EC109, KYSE-150, and KYSE-510 cells were obtained from the Thoracic Surgery Laboratory of West China Hospital of Sichuan University. The cells were cultured in RPMI 1640 with 10 % fetal bovine serum (FBS), 1 % penicillin/streptomycin, and 1 % L-glutamine. Cell culture flasks were maintained at 37 °C in an incubator with 5 % CO_2.

2.7. Cell transfection and lentiviral infection

shRNA lentivirus targeting VDR was constructed using lentivirus LV-VDR-RNAi (17,379–1) (GeneChem Company, Shanghai, Co. Ltd., Shanghai, China). In the function recovery experiment, we used the lentivirus LV-TP53-RNAi (82,797–11). The shRNA was synthesized and inserted into GV334 and GV298 lentivirus vector and verified by DNA sequencing according to the manufacturer's

Table 1
VDR expression in ESCC and adjacent normal tissues after immunohistochemistry staining.

		Adjacent normal tissues		Total	P value
		VDR low expression	VDR high expression		
ESCC tissues	VDR low expression	9	0	9	<0.001*
	VDR high expression	103	4	107	
Total		112	4	116	

ESCC, Esophageal squamous cell carcinoma; **VDR**, Vitamin D Receptor.* Meaningful P value.

instructions. After infection, we observed the cell condition and fluorescence expression rate using a fluorescence microscope. Only cells in good condition and with a fluorescence expression rate >80 % could be used to guide the formal infection experiment.

2.8. MTT assay

Cell proliferation was detected by adding 20 μL of 5 mg/mL MTT (Genview, USA) into a 96-well plate containing infected cells (2000 cells/well), which was incubated at 37 °C and 5 % CO_2 for five days. After dissolving with DMSO, the absorbance of each well was measured using a microplate reader with OD set at 490/570 nm. All experiments were performed in triplicate.

2.9. Apoptosis assay

According to the manufacturer's protocol, the infected cells were stained using an Annexin V/PI Cell Apoptosis kit (DOJIVDO, Japan) and apoptosis was analyzed by flow cytometry (FACS Calibur; BD Biosciences, San Jose, CA, USA). The assay was performed in triplicate.

2.10. Colony formation assay

Infected cells were plated at 500 cells/well in a 6-well plate and cultured in an incubator at 37 °C and 5 % CO_2 for nine days. The medium was changed every three days. After fixing with methanol, the colonies were stained with 0.1 % crystal violet (Sigma-Aldrich) for 20 min and washed with ddH2O. The number of colonies containing more than 50 cells was counted, and the assay was performed in triplicate.

2.11. Wound-healing assay

For the wound-healing assay, infected cells were seeded at a density of 50,000 cells/well in a 96-well plate and cultured until 90 % confluence. Cells were then scratched by the Celigo scratch instrument and treated with low-concentration serum medium (0.5 % FBS). At 8 h, 24 h, and 56 h after scratching and incubation, the migration area was analyzed with Celigo scanning (cat. No. VP408FH; V&P Scientific Inc). The assay was performed in triplicate.

2.12. Transwell assay

A 24-well cell culture insert with an 8-mm pore size (3422, Corning, USA) was used for Transwell assay. The insert coated with or without Matrigel (1:6 dilution; 354,234, Corning) was applied for the invasion or migration assay. First, a serum-free cell suspension was prepared on a 24-well plate, and the cells were counted to ensure that there were 105 cells/well. Then, 600 μL 30 % FBS RPMI 1640 medium was added to the lower chamber and cultured for 16 h and 24 h for the migration and invasion assays, respectively. A swab was then used to gently remove the nontransferred cells in the chamber, and the chamber was placed in 4 % paraformaldehyde fixative for 30 min. After fixation, GIEMSA staining solution or 0.5 % crystal violet water solution was applied to the lower surface of the membrane for 3 min for the migration and invasion assays, respectively. The membrane was sealed with neutral glue and observed with a microscope, and the cells were counted.

2.13. Tandem mass tag (TMT) quantification

In order to determine the potential molecular mechanism by which VDR promotes esophageal cancer tumorigenesis, we used TMT quantification to analyze the potential changes in downstream functional proteins and signaling pathways after VDR knockdown. We set up three knockdown groups, which included KYSE-150 cells infected by the VDR knockdown lentivirus. The three negative control groups included KYSE-150 cells infected with the negative control lentivirus.

2.13.1. Protein extraction, enzymatic hydrolysis, and peptide TMT labeling

We use the SDT lysis method [29] to lyse the sample and the Bradford method for protein quantification. One hundred micrograms of sample protein meeting the experimental requirements was diluted with 8 M urea buffer. The protein disulfide bond was then reduced by DTT, the sulfhydryl group was protected by IAA alkylation, and the Trypsin buffer was used for enzymatic hydrolysis after TEBA dilution. The peptides after enzymolysis were desalted by a Strata X C18 (phenomenex) desalting column, dried on a benchtop refrigerated vacuum concentrator (Concentrator Plus 5305, Eppendorf), and then frozen and stored for further TMT labeling. One hundred micrograms of peptides from each sample were labeled according to the TMT 6 plex Isobaric Mass Tag Labeling kit (Thermo Fisher Scientific).

2.13.2. Separation of peptide components and identification by mass spectrometry

The mixed labeled peptides were fractionated by an RP chromatography column (Waters, XBridge Peptide BEH C18 Column, 130 Å, 5 μm, 4.6 mm × 100 mm, 1/pkg) using an Agilent 1260 infinity II HPLC system. The eluted peptides were then collected for identification via mass spectrometry. Solvent B containing 0.1 % formic acid in 80 % acetonitrile had an increasing gradient from 6 % to 38 %, and then to 100 %, on an EASY-nLC 1000 UPLC system with 300 nL/min CFR. After chromatographic separation, the sample was

analyzed by a Q Exactive Plus mass spectrometer (Thermo Fisher Scientific). The scanning range of the precursor ion was 350–1800 *m/z*, the resolution of the primary mass spectrum was 70,000, and the ion dynamic exclusion time was 30 s. The normalized collision energy was set to 30 eV for intact fraction detection.

2.14. Parallel reaction monitoring (PRM)

PRM technology is based on the high-resolution and high-precision mass spectrometry platform represented by Orbitrap. First, the selection ability of the quadrupole mass analyzer was used to select the precursor ions of the target peptide with the quadrupole. The precursor ions were fragmented in the collision cell and the Orbitrap analyzer was used to detect all the precursor ions in the secondary mass spectrometer. Thus, relative/absolute quantification of the target protein/peptide was achieved.

2.14.1. LC-PRM analysis

After the enzymatically hydrolyzed peptides were desalted by the Strata X C18 desalting column, a hybrid Q Exactive Plus mass spectrometer (Thermo Fisher Scientific) coupled to a nano-EASY-nLC 1000 UPLC system (Thermo Fisher Scientific) was used to perform LC-PRM analysis. Solvent B containing 0.1 % formic acid in 80 % acetonitrile had an increasing gradient from 2 % to 40 %, and then to 90 %, on an EASY-nLC 1000 UPLC system with 300 nL/min CFR. After chromatographic separation, the sample was analyzed by a Q Exactive Plus mass spectrometer (Thermo Fisher Scientific). The scanning range of the precursor ion was 350–1500 *m/z*, the resolution of the primary mass spectrum was 70,000, and the ion dynamic exclusion time was 30 s. Normalized collision energy was set to 30 eV for intact fraction detection.

2.14.2. PRM precursor ion screening and detection

According to the results of LC-PRM analysis, the unique peptides of the protein to be tested were screened and included in the inclusion list by searching the Uniprot_HomoSapiens_20,367_20,200,226 database. Then, LC-PRM analysis was performed again with the following parameters: A, full-MS, scan range (*m/z*) = 350–1,500, resolution = 60,000, AGC target = 1e6, maximum injection time = 50 m s; and B, PRM, resolution = 15,000; AGC target = 1e5, maximum injection time = 50 m s, loop count = 14, isolation window = 1.6 *m/z*, NCE = 27 %.

2.14.3. Nude mouse tumor formation experiment (in vitro verification)

We selected 5-week-old female BALB/c nude mice for this experiment, which were provided by Beijing Weitong Lihua Laboratory Animal Technology Co., Ltd. Shanghai Branch (SCXK [Shanghai, China] 2017–0011). We selected the negative control virus-infected KYSE-150 cell line (inoculation amount: 2 E+06 cells/head) and the VDR knockdown lentivirus-infected KYSE-150 cell line (inoculation amount: 2 E+06 cells/head) for tail vein inoculation, and each group comprised 10 nude mice. D-Luciferin (15 mg/mL) was injected intraperitoneally at 10 μL/g. After the mice were anesthetized, they were placed under the intravital imaging device for imaging, and fluorescence expression was observed. The total radiant efficiency (p/s)/(μW/cm^2) was taken as the reference standard, which indirectly reflects the number of cells carrying fluorescent markers or the size of the tumor. Forty-two days after transplantation, the mice were euthanized with an overdose of 2 % sodium pentobarbital (0.5 mL). The mice were then dissected to observe whether there were tumor metastases in their lungs or other organs. The metastatic organs were removed to observe the fluorescence expression by intravital imaging, and fluorescence quantitative analysis was subsequently performed. All experimental procedures were approved by the institutional and local committee on the care and use of animals of West China Hospital of Sichuan University (Chengdu, China), and all animals received humane care according to the National Institutes of Health (USA) guidelines.

2.15. Statistical analysis

2.15.1. Clinicopathological characteristics analysis

The clinicopathological characteristics of the patients were analyzed by Pearson's chi-square test or Fisher's exact test to compare the dichotomous variables. Student's *t*-test was applied for the mean values of continuous variables that conformed to a normal distribution; the others were analyzed using the Mann-Whitney *U* test. Logistic regression analysis was performed to determine the important independent factors related to the level of VDR expression, and the multivariate logistic regression model only included variables with univariate *P*-values <0.05. Overall survival (OS) in patients was analyzed using Kaplan-Meier curves, and log-rank tests were used to determine the statistical significance. Multivariate survival analysis was carried out with the Cox proportional hazard regression model, in which the covariates that met the proportional hazards assumption of the covariate interaction test were considered to pass.

2.16. Proteomics data processing of TMT quantifications

LC-MS/MS raw files were processed using MASCOT engine (Matrix Science, London, UK; version 2.6) embedded into Proteome Discoverer 2.2, and the files were searched against the Uniprot_HomoSapiens_20,367_20,200,226 database downloaded from http://www.uniprot.org. The search parameters included trypsin as the enzyme used to generate peptides, with a maximum of two missed cleavages permitted. A precursor mass tolerance of 10 ppm and 0.05 Da tolerance for MS2 fragments were specified. A peptide and protein false discovery rate of 1 % was enforced using a reverse database search strategy [20]. Proteins with fold change >1.2 and P (Student's *t*-test) < 0.05 were considered differentially expressed proteins.

2.16.1. KEGG pathway annotation and subcellular localization analysis

All protein sequences were aligned to the Uniprot_HomoSapiens_20,367_20,200,226 database downloaded from NCBI (ncbi-blast-2.2.28+-win 32. exe), and only the sequences in the top 10 and with an E-value $\leq$ 1e-3 were kept. KEGG pathway annotation was performed using KEGG Orthology And Links Annotation (KOALA) software [30]. Fisher's exact test was used to enrich pathways by comparing the number of differentially expressed proteins and total proteins correlated to pathways. Meanwhile, WoLF PSORT [31] (https://wolfpsort.hgc.jp/) converts protein sequences into digital positioning features based on sorting signals, amino acid composition, and functional motifs, and then predicts the subcellular localization of the protein. Therefore, we used WoLF PSORT software to locate and predict the differential proteins.

2.16.2. Pathway and network analysis by ingenuity pathway analysis (IPA)

The list of differentially expressed genes from the results of TMT quantification was uploaded into the IPA software (version 42,012,434, Ingenuity Systems; Qiagen China Co., Ltd., China). The "core analysis" function included in the software was used to

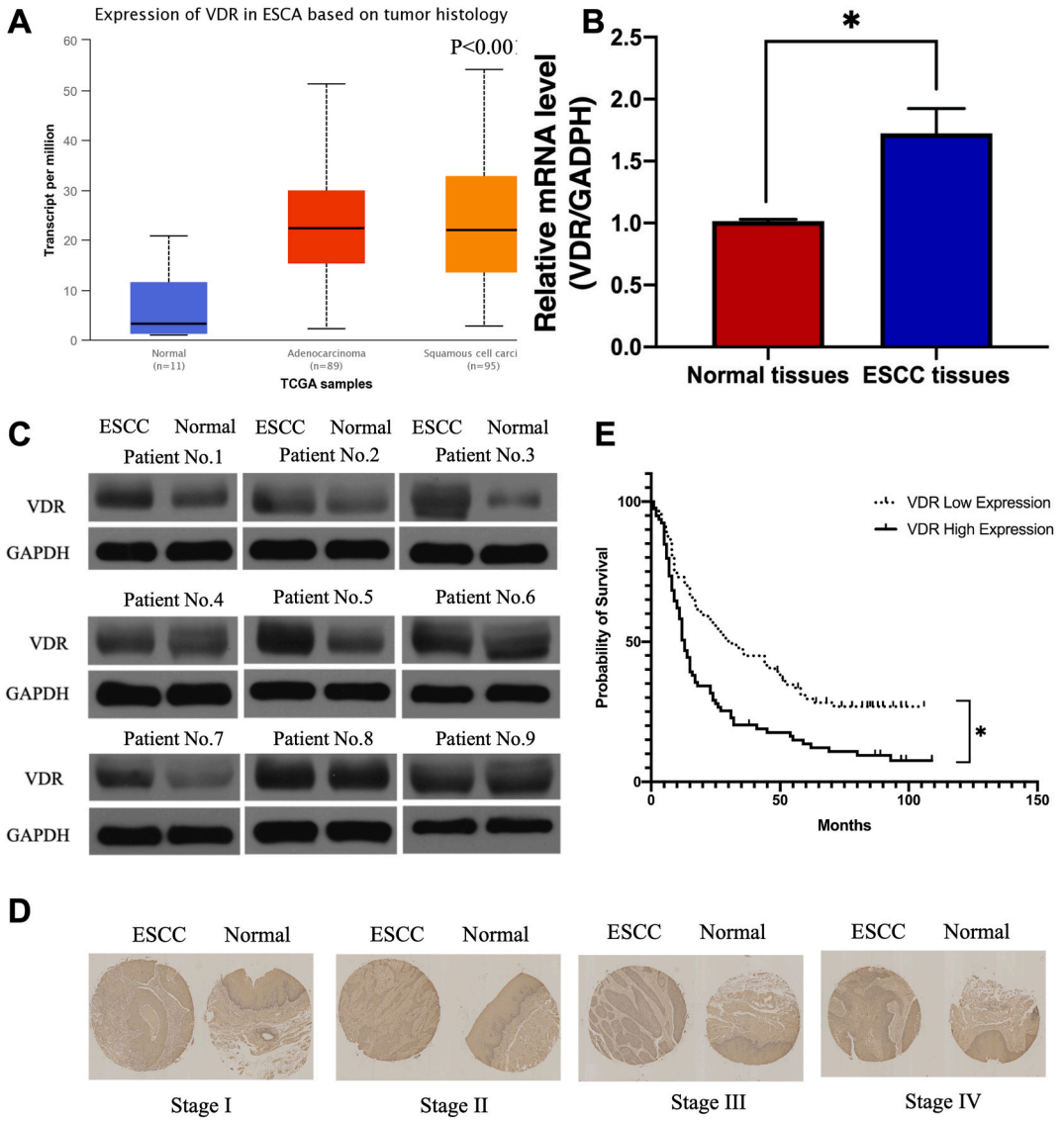

Fig. 1. Increased VDR expression is associated with poor prognosis of ESCC patients. (**A**) Relative RNA levels of VDR in ESCC and normal esophageal surface epithelium in the TCGA database. (**B**) Relative RNA levels of VDR in 20 pairs ESCC tissues and adjacent normal tissues assessed by RT-qPCR. (**C**) Western blot analysis of VDR expression in 9 pairs of fresh frozen ESCC specimens with related adjacent normal tissues. (**D**) Representative immunohistochemical images of VDR expression in stage I–IV ESCC tissues and adjacent normal tissues. (**E**) Kaplan-Meier analysis of ESCC of patients from ESCC TMA to observe correlations between VDR expression and overall survival. Data are shown as the means ± SD. *P < 0.05. ESCC, esophageal squamous cell carcinoma; RT-qPCR, reverse transcription-quantitative polymerase chain reaction; TCGA, The Cancer Genome Atlas; TMA, tissue microarray; VDR, vitamin D receptor.

interpret the differentially expressed data, which included biological processes, canonical pathways, upstream transcriptional regulators, and gene networks. Each gene identifier was mapped to its corresponding gene object in the ingenuity pathway knowledge base (IPKB).

3. Results

3.1. VDR is highly expressed in ESCC

To investigate the roles of VDR in ESCC development, we first analyzed the expression level of VDR through querying the TCGA-ESCA database. The expression of VDR in the 184 ESCC tissue samples was significantly higher than that in the 11 normal tissue samples (Fig. 1A). Then, the mRNA level of VDR in ESCC tissue was quantified in 20 pairs of fresh frozen ESCC specimens with related adjacent normal tissues collected from West China Hospital by RT-qPCR. Compared with adjacent normal tissues, the mRNA level of VDR in ESCC tissue was significantly higher (Fig. 1B). The Western blot results showed that VDR expression was higher in ESCC tissues compared with in adjacent normal tissues (Fig. 1C).

3.1.1. Higher VDR expression leads to poorer ESCC patient survival

To examine the expression of VDR in ESCC more precisely, we performed immunohistochemistry on ESCC TMA data, which contained 116 cases of ESCC and matched adjacent normal tissues and 73 single cases of ESCC. Fig. 1D shows the different expression of VDR in ESCC and adjacent normal tissues according to TNM stage. The expression of VDR was significantly higher in ESCC tissue compared to in adjacent tissues ($P < 0.001$, Table 1). The clinicopathological characteristics of VDR expression in ESCC TMA after scoring are listed in Table 2. VDR expression was also significantly different depending on gender ($P = 0.026$), T stage ($P = 0.002$), and TNM stage ($P = 0.044$). Moreover, according to logistic regression analysis, male gender ($P = 0.033$; OR = 0.459, 95 % CI: 0.224, 0.491), higher T stage ($P = 0.003$; OR = 2.652, 95 % CI: 1.382, 5.088), and higher TNM stage ($P = 0.041$; OR = 1.671, 95 % CI: 1.021, 2.735) are the independent risk factors related to higher VDR expression in ESCC (Table 3). In terms of survival, the median follow-up time was 16.3 months, which ranged from 1.0 to 108.6 months in our study. The mortality rate of patients during the follow-up period was 67.4 %, and the 5-year OS rate was 22.5 %. According to the Kaplan-Meier curves, the prognosis of ESCC patients with higher VDR expression was significantly worse ($P < 0.001$, Fig. 1E, HR = 1.911, 95 % CI: 1.361, 2.683, Table 4). After Cox multivariate regression analysis, VDR expression was shown to be an independent prognostic factor related to ESCC ($P = 0.002$; HR = 1.709, 95 % CI: 1.210, 2.413, Table 4).

3.1.1.1. VDR regulates ESCC cell proliferation, migration, and invasion. To explore the function of VDR in ESCC, we sought to determine the altered cell phenotypes in ESCC cells that had overexpressed or depleted VDR. First, the results of RT-qPCR show that VDR had significantly higher expression in KYSE-410, TE-1, EC109, KYSE-150, and KYSE-510 cells compared to in the normal esophageal epithelial cell line, Het-1a (Fig. 2A). Among them, VDR expression was the highest in KYSE-150 cells, followed by in KYSE-410 cells,

Table 2
Clinicopathological characteristics of VDR expression on ESCC tissue microarray.

		VDR low expression 89 (%)	VDR high expression 80 (%)	P
Gender	Male	57 (47.1)	64 (52.9)	0.026*
	Female	32 (66.7)	16 (33.3)	
Age	<55	15 (42.9)	20 (57.1)	0.133
	≥55	74 (55.2)	60 (44.8)	
Tumor location	Upper thoracic	7 (70.0)	3 (30.0)	0.441
	Middle thoracic	64 (52.9)	57 (47.1)	
	Lower Thoracic	18 (47.4)	20 (52.6)	
T stage	T1	5 (62.5)	3 (37.5)	0.002*
	T2	27 (79.4)	7 (20.6)	
	T3	57 (45.6)	68 (54.4)	
	T4	0 (0.0)	2 (100.0)	
N stage	N0	50 (60.2)	33 (39.8)	0.275
	N1	22 (44.0)	28 (56.0)	
	N2	13 (46.4)	15 (53.6)	
	N3	4 (50.0)	4 (50.0)	
M stage	M0	86 (52.4)	78 (47.6)	0.550
	M1	3 (60.0)	2 (40.0)	
TNM stage	I	7 (70.0)	3 (30.0)	0.044*
	II	47 (61.8)	29 (38.2)	
	III	32 (41.0)	46 (59.0)	
	IV	3 (60.0)	2 (40.0)	
Differentiation	High	12 (66.7)	6 (33.3)	0.160
	Moderate	72 (52.9)	64 (47.1)	
	Low	5 (33.3)	10 (66.7)	

ESCC, Esophageal squamous cell carcinoma; **VDR**, Vitamin D Receptor; * Meaningful P value.

Table 3
Univariate and multivariate logistic regression analyses of VDR expression in ESCC patients.

	Univariate regression analysis			Multivariate regression analysis			Multivariate regression analysis		
	OR	95%CI	P	OR	95%CI	P	OR	95%CI	P
Gender	0.445	0.222, 0.895	0.023*	0.459	0.224, 0.941	0.033*	0.492	0.241, 1.002	0.051
Age	0.608	0.287, 1.289	0.194						
Tumor location	1.418	0.776, 2.591	0.257						
T stage	2.673	1.414, 5.056	0.002*	2.652	1.382, 5.088	0.003*			
N stage	1.290	0.915, 1.819	0.146						
M stage	0.735	0.120, 4.515	0.740						
TNM stage	1.786	1.100, 2.901	0.019*				1.671	1.021, 2.735	0.041*
Differentiation	1.986	0.962, 4.099	0.064						

95%CI, 95 % Confidence Interval**; ESCC**, Esophageal squamous cell carcinoma; **OR:** Odds Ratio**; VDR**, Vitamin D Receptor; * Meaningful P value.

Table 4
Univariate and multivariate Cox regression analyses of clinical factors associated with 5-year overall survival on ESCC tissue microarray.

	Univariate Cox regression analysis			Multivariate Cox regression analysis			Multivariate Cox regression analysis		
	HR	95%CI	P	HR	95%CI	P	HR	95%CI	P
Gender	0.459	0.303, 0.695	<0.001*	0.605	0.395, 0.927	0.021*	0.599	0.391, 0.916	0.018*
Age	0.813	0.544, 1.214	0.311						
Tumor location	1.146	0.835, 1.572	0.398						
T stage	1.825	1.300, 2.562	0.001*	1.430	1.000, 2.045	0.050*			
N stage	1.735	1.436, 2.097	<0.001*	1.613	1.325, 1.965	<0.001*			
M stage	2.455	0.998, 6.040	0.051						
TNM stage	2.309	1.754, 3.039	<0.001*				2.206	1.651, 2.946	<0.001*
Differentiation	1.044	0.710, 1.536	0.826						
VDR expression	1.911	1.361, 2.683	<0.001*	1.665	1.169, 2.370	0.005*	1.709	1.210, 2.413	0.002*

95%CI, 95 % Confidence Interval**; ESCC**, Esophageal squamous cell carcinoma; **HR:** Hazard Ratio**; VDR**, Vitamin D Receptor; * Meaningful P value.

and VDR expression was relatively low in TE-1, EC109, and KYSE-510 cells. Meanwhile, Western blot results (Fig. 2A) verified the results of RT-qPCR. VDR was efficiently knocked down and overexpressed by two lentiviruses in the KYSE-150 and KYSE-510 cell lines, respectively (Fig. 2B).

MTT assay showed significantly decreased ($P = 0.00016$) cell proliferation in the VDR knockdown group; however, cell proliferation increased significantly in the VDR overexpression group ($P = 0.00875$) (Fig. 2C). Similarly, the results of the colony formation assay also indicate that the clonogenic capacity of the VDR knockdown group was significantly inhibited compared with that in the negative control group ($P = 0.00106$), while the number of cell clones in the VDR overexpression group was significantly increased ($P = 0.00112$) (Fig. 2D).

3.1.1.2. VDR inhibits ESCC cell apoptosis. VDR deficiency could induce apoptosis in KYSE-150 cells ($P < 0.001$). Meanwhile, the apoptotic rate of the VDR overexpression group was less than 5 %, which was therefore, regarded as having no obvious apoptosis (Fig. 2E).

3.1.2. VDR promotes ESCC invasion and metastasis

The wound-healing assay indicated that the migration capacity of ESCC cells was remarkably inhibited upon VDR knockdown, and it could be salvaged after VDR overexpression (Fig. 2F). Furthermore, the Transwell assay also demonstrated that VDR knockdown impaired the migration and invasion abilities of KYSE-150 cells (Fig. 2G), while the cell phenotypes could be reversed after VDR overexpression (Fig. 2H).

3.1.3. Vitamin D down-regulates VDR expression and inhibits the ESCC cell progression

To explore the relationship between vitamin D and VDR, KYSE-150 cells were treated with calcitriol at the indicated concentrations. Upon calcitriol treatment, the expression of VDR was gradually reduced, as shown by RT-qPCR and western blotting (Fig. 3A and B). We next examined whether treatment with calcitriol further inhibited tumorigenesis of ESCC cells based on VDR depletion. As shown in Fig. 3C and D, calcitriol treatment resulted in a significant decrease in the proliferation of KYSE 150 cells with VDR knockdown ($P < 0.001$).

3.1.4. Identification of differentially expressed proteins after VDR knockdown by LC-MS/MS-TMT

To explore the underlying mechanisms of VDR in ESCC development, we first performed a quantitative analysis of downstream differentially expressed proteins using LC/LC-MS and TMT with VDR knockdown. Three pairs of VDR knockdown and control groups were used in this study (Fig. 4A). We identified 7586 peptides through spectral analysis, of which 99.4 % were unique. Principal component analysis (PCA) was performed to verify the quantitative results of the triplicate samples. Better repeatability was found

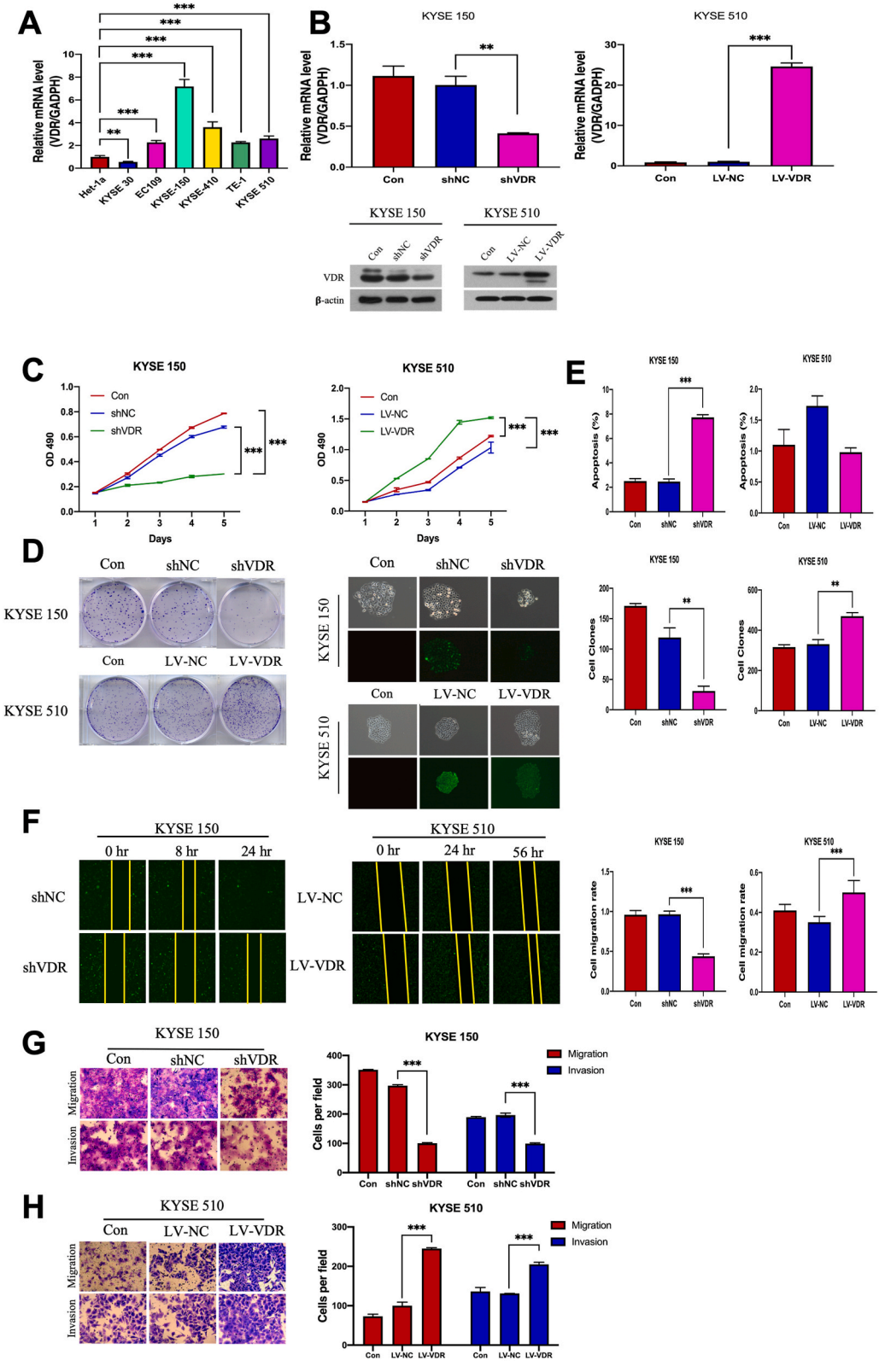

(caption on next page)

Fig. 2. VDR regulates cell growth and migration in vitro. (A) RT-qPCR and Western blot analysis of VDR expression in ESCC cell lines and an esophageal surface epithelium cell line (Het-1a). **(B)** RT-qPCR and Western blot analysis of VDR expression in KYSE-150 and KYSE-510 cells infected with shRNA and overexpression lentivirus targeting VDR or a control shRNA and a control lentivirus. **(C)** MTT assays were performed to determine cell growth after VDR knockdown in KYSE-150 cells and overexpression in KYSE-510 cells. **(D)** Colony formation assay of the KYSE-150 and KYSR-510 cells described in (B). **(E)** VDR deficiency could induce KYSE-150 cell apoptosis, but no obvious apoptosis occurred after VDR overexpression in KYSE-510 cells. **(F)** Wound-healing assay showed VDR promotes ESCC cell migration. **(G)** VDR knockdown decreased the migration and invasion abilities of KYSE-150 cells. **(H)** VDR overexpression increased the migration and invasion abilities of KYSE-510 cells. Data are shown as the mean ± SD. *P < 0.05, **P < 0.01, ***P < 0.001. ESCC, esophageal squamous cell carcinoma; RT-qPCR, reverse transcription-quantitative polymerase chain reaction; NC, Negative Control; shRNA, short hairpin RNA; LV, lentivirus; VDR, vitamin D receptor.

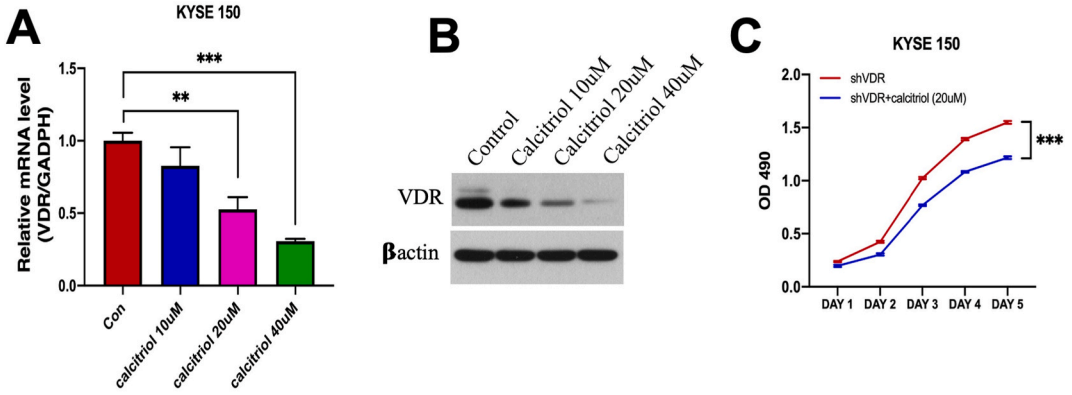

Fig. 3. Calcitriol down-regulates VDR in ESCC cells and further inhibits the ESCC cell growth with VDR depletion. (**A-B)** RT-qPCR and Western blot analysis of VDR expression in KYSE-150 cells treated with calcitriol at indicated concentrations (10-40μM, 24 h). **(C)** MTT assay was performed to determine cell growth after calcitriol treatment in KYSE-150 cells with VDR deficiency. Data are shown as the mean ± SD. *P < 0.05, **P < 0.01, ***P < 0.001. ESCC, esophageal squamous cell carcinoma; RT-qPCR, reverse transcription-quantitative polymerase chain reaction; VDR, vitamin D receptor.

between the KYSE-150 knockdown group and negative control groups according to PCA (Fig. 4B). The relative standard deviation (RSD) distribution showed that the quantitative evaluation of proteins between the two groups was comparable, with low variability. Differentially expressed proteins were defined as having P < 0.05, or log 2-fold changes >1.2. Finally, VDR knockdown resulted in the global alteration of 984 proteins, including 639 upregulated and 345 downregulated proteins (Fig. 4C and D).

KEGG pathway annotation and subcellular localization analysis of identified differentially expressed proteins.

KEGG pathway annotation analysis showed that the differentially expressed proteins after VDR knockdown were mainly enriched in complement and coagulation cascades (enrichment of 19 differential proteins), which may indicate that angiogenesis is promoted and blood circulation around the tumor is relatively blocked. In addition, ferroptosis (enrichment of 12 differential proteins) and the p53 signaling pathway (enrichment of 13 differential proteins) were also in the top 10 pathways according to KEGG annotation (Fig. 4E). Subcellular localization analysis showed that most of the differentially expressed proteins enriched after VDR knockdown were localized in the nucleus (29.0 %) and cytoplasm (24.8 %), followed by the plasma membrane (16.6 %), extracellular space (14.4 %), and mitochondria (11.3 %) (Fig. 4F). The 11.3 % protein value from the mitochondria indicated the potential for mitochondrial-mediated oxidative stress regulation between the KYSE-150 shNC and shVDR groups. As an important tumor suppressor, p53 can induce cell apoptosis [32], and it has also been confirmed that p53 family members can directly regulate VDR [33,34]. However, we further investigated whether VDR can inversely regulate p53 expression and how VDR promotes tumorigenesis through IPA.

3.1.5. Enriched biological pathway and function analysis by IPA

To determine the most significant canonical pathways and biological networks related to VDR depletion, we applied IPA, followed by TMT quantification. For analysis of the canonical pathways, disease, and function, a −log (*P*-value) > 2 was considered as the threshold, Z-score >2 was defined as the threshold of significant activation, and Z-score <−2 was defined as the threshold of significant inhibition. For upstream regulators, a *P*-value of overlap <0.05 was set as the threshold. IPA revealed a highly significant overlap of 192 canonical pathways (P < 0.05) related to apoptosis, cancer, cell cycle regulation, cellular immune response, cellular growth, and proliferation. Among them, LXR/RXR activation was predicted to be significant, with a Z-score of 3.638. Meanwhile, p53 signaling observed via KEGG pathway annotation was also activated in IPA, with a Z-score of 0.378. The most significant classical pathways related to VDR knockdown are shown in Fig. 4G. Based on previous studies, apolipoprotein E (APOE) in LXR/RXR activation and TP53 in p53 signaling were selected as functional proteins for future studies.

Prediction of the upstream regulatory factors showed that lipopolysaccharide is strongly activated, showing activation in 105 activated and 31 inhibited genes, with a total of 453 upstream regulatory factors regulating TP53. To evaluate the positive correlation between VDR and other diseases, we compared the differentially expressed genes of VDR with other disease gene sets. VDR was mostly

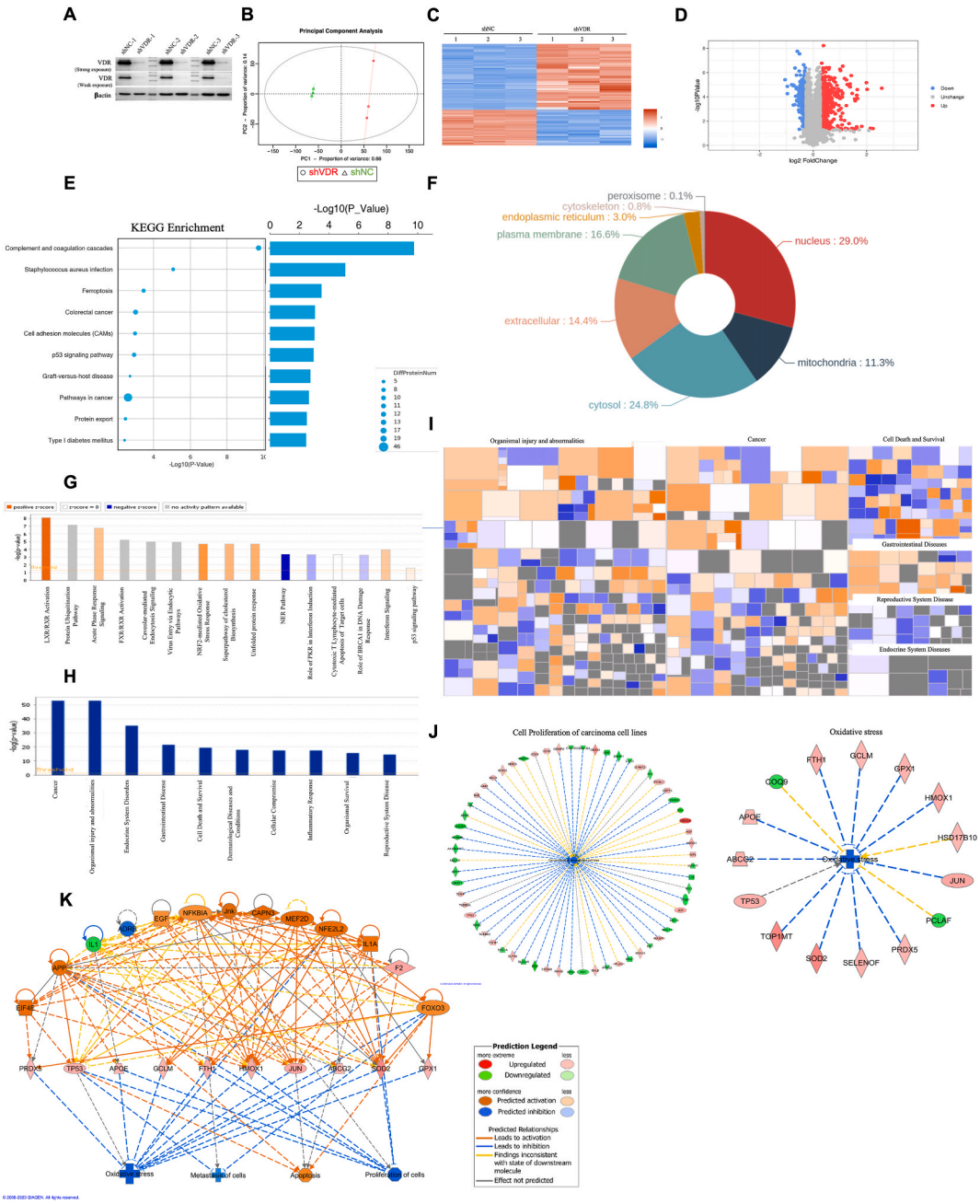

Fig. 4. Identification of the VDR targets in ESCC cells. (A) Western blot analysis of VDR expression in KYSE-150 cells infected with shRNA lentivirus targeting VDR or a control shRNA in triplicate. **(B)** Principal component analysis showed the better repeatability between the VDR knockdown group and the control group in KYSE-150 cells. **(C)** Heatmap of differentially expressed genes identified by TMT quantification after VDR knockdown. **(D)** Volcano plot of gene expression changes associated with VDR deficiency. **(E)** KEGG enrichment analysis of differentially expressed genes. **(F)** Subcellular localization analysis of differentially expressed genes. **(G)** Plot of a total of 15 representative classifications of canonical pathways possibly related to VDR depletion. **(H)** Classification of 10 possible representative diseases and functions mediated by VDR in ESCC development and function. (G and H: categories are shown in terms of the -log (*P*-value) [left y-axis] and the number of differentially expressed genes counted [right y-axis]). **(I)** Heatmap representing the classification of diseases and functions. This heatmap was drafted according to its Z-score values; higher Z-scores represented by orange indicate activation, whilst lower Z-scores represented by blue indicate inhibition. **(J)** Gene networks of carcinoma cell proliferation and oxidative stress associated with VDR knockdown. **(K)** Network diagram representing the regulatory effects with top consistency scores. After VDR knockdown, the top network, which yielded a consistency score = 14.230, was "Oxidative stress". Regulation of cell proliferation, apoptosis, and metastasis were also added. ESCC, esophageal squamous cell carcinoma; KEGG, Kyoto Encyclopedia of Genes and Genomes; NC, Negative Control; shRNA, short hairpin RNA; TMT, tandem mass tag; VDR, vitamin D receptor. (For interpretation of the references to colour in this figure legend, the reader is referred to the Web version of this article.)

involved in cancer, organismal injury, and abnormalities (Fig. 4H and I). Apoptosis of carcinoma cell lines (Z-score = 0.761) was predicted to be activated, metastasis of tumor cell lines (Z-score = −0.926) was predicted to be inhibited, and oxidative stress (Z-score = −2.175) and proliferation of carcinoma cell lines (Z-score = −2.026) were predicted to be significantly inhibited (Fig. 4J).

3.2. Regulatory effects based on IPA

Consistency scores were calculated to observe the regulatory effects and molecular networks. A high consistency score indicates accurate results for the regulatory effect analysis. Finally, by integrating the results of canonical pathways, upstream regulatory factors, differential gene datasets, and the diseases and functions predicted through IPA, we observed a highly significant overlap of 52 regulatory networks related to VDR knockdown. The top regulatory networks showing upstream regulators included ADRB, APP, CAPN3, EGF, EIF4E, F2, FOXO3, IL1, IL1A, Jnk, MEF2D, NFE2L2, and NFKBIA. These may activate apoptosis by regulating genes such as ABCG2, APOE, FTH1, GCLM, GPX1, HMOX1, JUN, PRDX5, SOD2, and TP53, and inhibit oxidative stress, cell metastasis, and cell proliferation (consistency score = 14.230) (Fig. 4K).

Parallel reaction monitoring (PRM) analysis, Western blot verification, and function recovery experiment.

To verify the differentially expressed proteins in the regulatory network of oxidative stress identified through IPA, ABCG2, APOE, FTH1, GCLM, GPX1, HMOX1, JUN, PRDX5, SOD2, and TP53 were selected for absolute differential protein quantitative analysis using PRM. The TMT results and peptides are presented in Tables 5 and 6, respectively. The results suggested that TP53 was upregulated after VDR knockdown in the KYSE-150 cell line; FTH1, GCLM, GPX1, and SOD2 were also upregulated (Table 7). Compared with the negative control group, the expression of TP53 and APOE was upregulated after VDR knockdown. SOD2 and JUN, which are reported to be related to oxidative stress, were also confirmed to be upregulated via western blotting (Fig. 5A). Subsequently, we verified whether the opposite results were observed after knocking down TP53 under VDR knockdown conditions. First, TP53 was significantly knocked down alongside VDR knockdown in KYSE-150 cells, and the TP53 knockdown efficiency in the shVDR + shTP53 group was 84.3 % ($P < 0.001$) (Fig. 5B and C). Western blotting verified the RT-qPCR results (Fig. 5D). According to functional recovery experiments, TP53 knockdown significantly reversed the inhibition of cell proliferation mediated by VDR knockdown, as determined by the MTT assay in KYSE-150 cells (Fig. 5E). Similarly, the results of the colony formation assay revealed that the capacity of cell clones inhibited after VDR knockdown was also reduced by TP53 knockdown (Fig. 5F–H), indicating that VDR may inhibit TP53 expression to promote ESCC development.

3.2.1. VDR deficiency inhibits the growth and metastasis of esophageal cancer in nude mice

To verify whether VDR knockdown inhibited the proliferation and metastasis of ESCC cells in vivo, VDR-deficient KYSE-150 ESCC cells and control cells were injected through the tail vein to construct a peritoneal metastatic xenograft model in 5-week-old female BALB/c nude mice. Each group contained ten nude mice. The results of in vivo imaging are shown in Fig. 5I, wherein the total fluorescence expression in the average area of the negative control group and the VDR knockdown group ([p/s]/[μW/cm^2]) were 1.27 E+08 ± 1.34 E+08 and 3.77 E+06 ± 74.54 E+06 ($P = 0.01725$), respectively (Fig. 5J). Compared with the negative control group, fluorescence expression decreased in mice in the VDR knockdown group, indicating that tumorigenesis was reduced in the mice in the VDR knockdown group. The mice were sacrificed to evaluate tumor metastasis 42 days after transplantation. As shown in Fig. 5K, the number of lung and subcutaneous metastases in the VDR knockdown group was significantly reduced compared with that in the negative control group.

4. Discussion

VDR is a nuclear transcription factor of the steroid hormone receptor family. Furthermore, it has been reported that VDR promotes cell apoptosis and differentiation and inhibits cell proliferation by binding to vitamin D in blood [12,13,35]. However, the specific biological function and mechanism of epigenetic regulation of VDR in esophageal cancer has not been widely explored.

In this study, VDR was highly expressed in ESCC tissues, and we confirmed previous results reporting that VDR is mostly expressed in the cytoplasm [36–40]. VDR mRNA expression has also been previously reported in esophageal adenocarcinoma and Barrett's

Table 5
Quantification and difference analysis of proteins involved in Oxidative stress after TMT proteomics.

Gene Name	Average shVDR	Average shNC	Regulation	shVDR/shNC	P value
ABCG2	116.3667	83.63333	UP	1.391391	0.002507*
APOE	112.8333	87.2	UP	1.29396	0.000946*
FTH1	117.8	82.2	UP	1.43309	1.06E-05*
GCLM	113.2667	86.73333	UP	1.305919	5.98E-09*
GPX1	115.5667	84.43333	UP	1.368733	2.01E-06*
HMOX1	119.5	80.46667	UP	1.485087	2.8E-05*
JUN	122.5	77.53333	UP	1.579966	0.000308*
PRDX5	112.2333	87.76667	UP	1.278769	0.000192*
SOD2	136.5667	63.43333	UP	2.152916	2.98E-07*
TP53	118.0333	82	UP	1.439431	1.38E-05*

NC, Negative Control**; shRNA**, short hairpin RNA; **TMT**, Tandem Mass Tags**; VDR**, Vitamin D Receptor; * Meaningful P value.

Table 6
PRM target peptide list.

Master Protein Accessions	Gene Name	Annotated Sequence	Charge	*m/z*	RT [min]
P02794	FTH1	YFLHQSHEER	2	673.318	8.691
P02794	FTH1	NVNQSLLELHK	3	432.242	21.252
P02794	FTH1	QNYHQDSEAAINR	2	773.356	10.472
P48507	GCLM	TLNEWSSQINPDLVR	2	886.459	42.784
P48507	GCLM	LFIVESNSSSSTR	2	713.863	24.155
P07203	GPX1	YVRPGGGFEPNFMLFEK	3	663.326	47.633
P07203	GPX1	DYTQMNELQR	2	649.299	26.275
P30044	PRDX5	VGDAIPAVEVFEGEPGNK	3	609.979	44.627
P30044	PRDX5	THLPGFVEQAEALK	3	513.947	35.410
P30044	PRDX5	FSMVVQDGIVK	2	611.832	34.985
P30044	PRDX5	VNLAELFK	2	467.276	43.364
P04179	SOD2	GDVTAQIALQPALK	2	712.909	32.332
P04179	SOD2	HHAAYVNNLNVTEEK	2	869.929	13.994
P04637	TP53	TCPVQLWVDSTPPPGTR	2	955.975	39.728

PRM, Parallel Reaction Monitoring.

Table 7
PRM protein absolute quantification result.

Protein Accessions	Gene Name	Average shVDR	Average shNC	shVDR/shNC	P value
P02794	FTH1	247897.3	147681.6	1.678593	2.24E-04*
P48507	GCLM	1,478,770	709664.5	2.083759	6.81E-04*
P07203	GPX1	171134.5	104772.3	1.633395	2.87E-02*
P30044	PRDX5	196443.1	168926.9	1.162888	3.94E-01*
P04179	SOD2	964219.2	291775.5	3.304662	2.72E-02*
P04637	TP53	508204.3	345624.6	1.470394	1.83E-01*

PRM, Parallel Reaction Monitoring**; NC,** Negative Control**; shRNA**, short hairpin RNA; **VDR**, Vitamin D Receptor; * Meaningful P value.

esophagus [25]; meanwhile, VDR expression has rarely been reported in ESCC. In a previous study, high VDR expression was not detected in ESCC through immunohistochemistry, and only 1 % of normal specimens had high VDR expression [25]. Bao et al. reported that VDR expression was higher in tumor cells than in stromal cells, but there was no significant difference in VDR expression between normal and ESCC tissue at the mRNA level [26]. In our study, VDR was more highly expressed at a higher T stage and in more advanced esophageal cancer, and VDR expression in ESCC was shown to be an independent risk factor related to prognosis. However, VDR expression decreased in highly malignant tumors, which is in agreement with the results obtained by Zhou et al. [25]. Studies on colon cancer [15,20,41] have reported that the number of VDR-positive colon cells increases significantly with tumor progression, and this number reaches its maximum in low-grade adenocarcinoma; meanwhile, in highly malignant tumors, the number of VDR-positive colon cells decreases. These results suggest that in addition to the interaction between vitamin D and VDR, high VDR expression is more likely to induce cancer tumorigenesis. The results observed in the TCGA database also confirm these results.

Different studies have come to different conclusions regarding the effect of VDR expression on esophageal cancer prognosis. Our study confirmed that VDR is an independent risk factor related to the prognosis of ESCC. Some results in ovarian cancer [40] and esophageal adenocarcinoma support these findings [25]; however, other studies have obtained contradictory results. Stephen et al. first proposed that there is a significant dose-response relationship between higher VDR expression and improved survival in patients with esophageal adenocarcinoma [42,43]. There are many differences in the design of this study compared to our study, which may be the reason for these contradictory results. In our study and the study by Zhou et al. all patients were not exposed to neoadjuvant therapy before surgery, avoiding the effect of neoadjuvant therapy on VDR expression. However, in the study by Stephen et al. all patients received neoadjuvant therapy before surgery. A small study of 15 patients found that patients with higher VDR expression responded less to neoadjuvant treatment, indicating a potential interaction between neoadjuvant therapy and VDR expression [42]. Moreover, the study population (Northern Ireland and China) may be fundamentally different between different studies. Additionally, the studies used different antibodies to stain the specimens. All these factors may explain the differences in the results to some extent. At the same time, a previous study also reported that vitamin D may stimulate VDR expression; after combining with vitamin D, they can promote cell apoptosis and differentiation and inhibit cell proliferation in various malignant cells. Moreover, our previous study confirmed that the plasma vitamin D level in patients with esophageal cancer was lower than that in normal individuals, and that the vitamin D level decreased with esophageal cancer progression [3]. It can be deduced that the vitamin D level continues to decrease as esophageal cancer progresses, while the expression of uncombined VDR increases. These findings explain why VDR expression was higher in esophageal cancer tissues than in normal tissues in our study. Meanwhile, with the relative increase in the amount of uncombined VDR, the true effect of VDR on esophageal cancer tumorigenesis is gradually revealed. Thus, VDR promotes the progression of esophageal cancer and adversely affects patient prognosis.

The relative and absolute quantitative isotope labeling TMT technology can flexibly compare the relative and absolute content of proteins in up to 10 different samples. In recent years, it has been recognized as a powerful method for discovering new disease

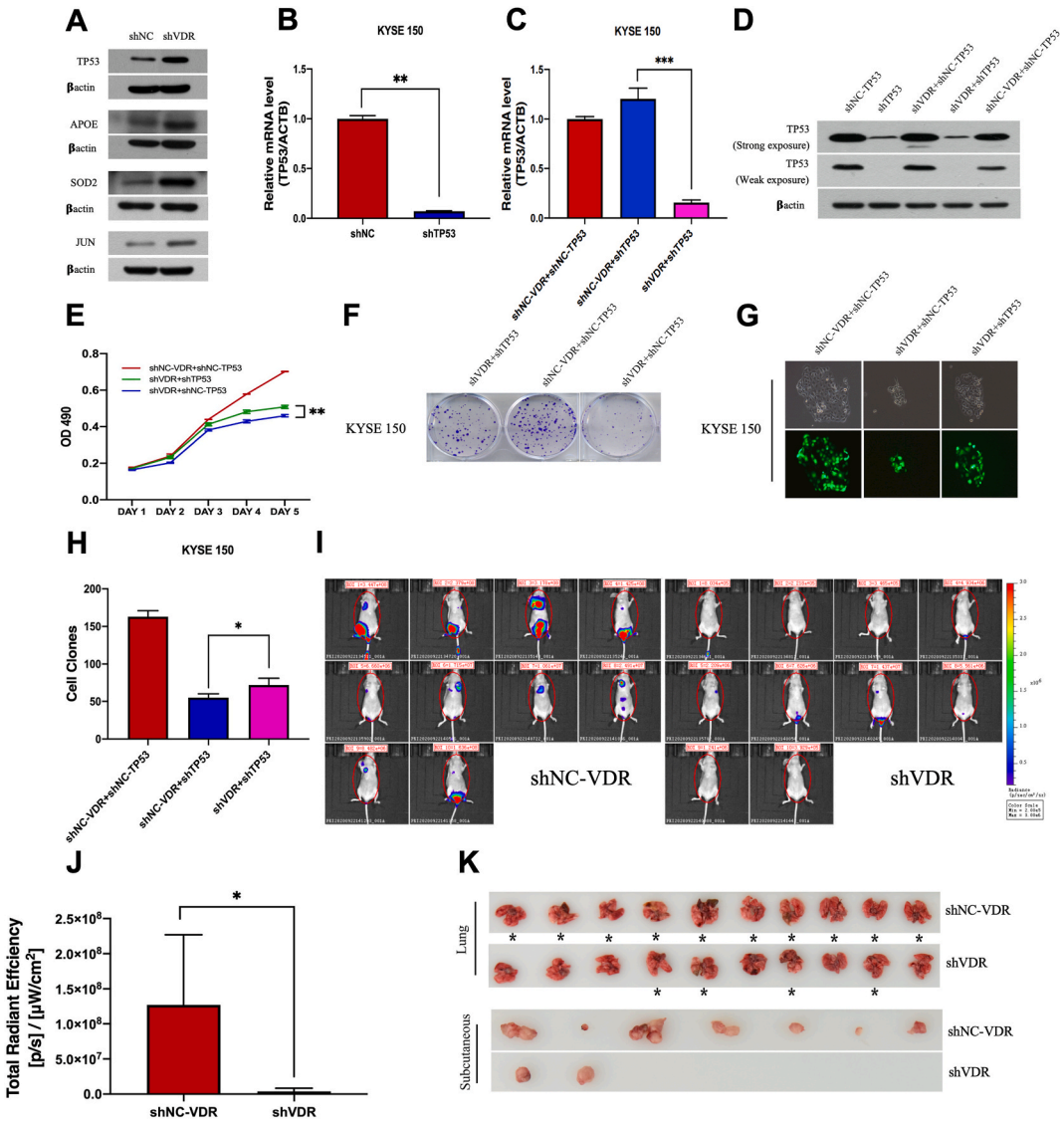

Fig. 5. Identification of the VDR targets in ESCC cells. **(A)** Expression levels of four selected proteins were validated by western blotting. **(B–D)** RT-qPCR and Western blot analysis for VDR and TP53 expression in VDR-deficient KYSE-150 cells upon TP53 knockdown. **(E–H)** Cell growth was measured by MTT assays (E) and colony formation assays in KYSE-150 cells (F–H). **(I–J)** Inhibition of VDR impaired the growth of xenografted tumors. Representative images and quantification of fluorescence expression in vivo imaging are shown. **(K)** Tumor metastasis was measured 42 days after transplantation by dissecting the organs from the nude mice of each group and photographed. Data are shown as the mean ± SD. *P < 0.05/metastases observed, **P < 0.01, ***P < 0.001. ESCC, esophageal squamous cell carcinoma; RT-qPCR, reverse transcription-quantitative polymerase chain reaction; NC, Negative Control; shRNA, short hairpin RNA; VDR, vitamin D receptor.

biomarkers [44,45]. In this study, to elucidate the potential regulatory effect of VDR in ESCC, we applied TMT labeling and LC-MS/MS to perform proteomic quantitative analysis on three VDR knockdown groups and three negative control groups, respectively. After VDR knockdown, a total of 984 differentially expressed genes were identified, of which 639 were upregulated and 345 were down-regulated. We subsequently included the differential proteins in KEGG enrichment annotation analysis. Based on the top 10 pathways with the most differential protein enrichment, 13 differential proteins were enriched in the p53 signaling pathway. Combined with previous studies, the tumor suppressor gene p53 plays a variety of roles in regulating cell cycle progression, apoptosis, autophagy, differentiation, aging, and DNA repair, and it also affects cell metabolism and cytokines [46]. P53 is also the tumor suppressor gene that is most closely related to human esophageal cancer. The most important function of p53 is to maintain chromosome stability [47, 48]. Studies have shown that abnormalities in p53 can be found in 40–60 % of esophageal cancer patients [49]. In this study, the protein enrichment of the p53 signaling pathway was significantly higher (P = 0.00114, FDR: 0.0382) after VDR knockdown, and the expression of TP53 was significantly increased (shVDR/shNC: 1.4394, P < 0.001). Therefore, we chose to explore the changes in cell function after VDR knockdown by conducting further research on TP53 and the p53 signaling pathway.

We then applied the IPA system to reveal the signal transduction pathways, interactions, and functional effects that mediate changes in cell function related to VDR knockdown. The results of classical pathway analysis indicate that VDR may be involved in 234 classical signaling pathways, among which the "LXR/RXR activation" pathway (Z-score = 3.638) is considered to be the highest-level signaling pathway. LXR/RXR is a ligand-dependent transcription factor and is closely related to nuclear receptors, such as PPAR and FXR. The transcriptional activity of LXRs (two isoforms, LXRα and LXRβ) depends on the formation of heterodimers with RXRs [50,51]. The p53 signaling pathway (Z-score = 0.378 > 0) was also shown to be activated according to IPA. These findings may provide resources for exploring disease treatment strategies that use VDR as a molecular target. By integrating the results of IPA, we identified the regulatory effects on the upstream regulatory network involved in differential genes after VDR knockdown, in addition to the possible pathways of downstream diseases and functions.

IPA predicted a total of 52 regulatory effects, among which Oxidative stress yielded a high consistency score. Oxidative stress is a cellular state wherein the level of reactive oxygen species (ROS) in the cell exceeds its antioxidant defense mechanism. Several studies have confirmed that there is a strong relationship between oxidative stress and the formation or progression of several human diseases, including cancer [52–54]. Epidemiological studies have also connected chronic oxidative stress with cancer [55]; therefore, the involvement of oxidative stress in cancer progression has been recognized. ROS are produced during normal cell metabolism, but excessive ROS damage the genome and mitochondrial DNA, leading to DNA damage, molecular mutations, and changes in signaling pathways. Both endogenous and exogenous drugs have been shown to induce an increase in ROS. If these ROS are not detoxified by antioxidants, they may lead to an increase in oxidative stress in cells. If the oxidative stress is severe enough, it will change the structure and function of key cellular macromolecules and promote tumor formation. The production of mitochondrial ROS and the resulting tumor induction have been demonstrated [56,57]. The differential genes that coregulate oxidative stress with TP53 are as follows: APOE, ABCG2, FTH1, GCLM, GPX1, HMOX1, JUN, PRDX5, and SOD2. It was confirmed by PRM and Western blot that the expression of TP53, SOD2, APOE, FTH1, GCLM, GPX1, PRDX5, and JUN were upregulated after VDR knockdown. These genes belong to many different signaling pathways, including NRF2-mediated oxidative stress (FTH1, GCLM, SOD2, JUN), glutathione redox reaction I (GPX1), mitochondrial dysfunction (PRDX5), the p53 signaling pathway (TP53), and LXR/RXR activation (APOE). Notably, the expression of the antioxidants SOD2, PRDX5, GPX1, and GCLM increased significantly after VDR knockdown. These findings suggest that the upregulation of APOE, SOD2, PRDX5, GPX1, and GCLM expression after VDR knockdown may inhibit oxidative stress, resulting in a significant decrease in KYSE-150 cell proliferation. In addition, the upregulated TP53 also plays a separate role in inhibiting oxidative stress, tumor metastasis, and promoting tumor apoptosis. Meanwhile, p53 has been reported to have a low to moderate oxidative stress level. Under the circumstances of radiation, hypoxia, and oxidants, p53 induces apoptosis by initiating DNA fragmentation, which promotes the increase of cell pressure and thereby, prevents the proliferation of abnormal cells [58]. We have confirmed that silencing VDR expression resulted in upregulation of TP53 expression, while contradictory results were obtained upon TP53 knockdown in VDR-deficient ESCC cells. Based on these results and the inhibitory effect of exogenous VDR knockdown on oxidative stress, our study suggests that the p53 signaling pathway is activated after VDR knockdown, which in turn inhibits tumor oxidative stress and prevents the development of ESCC.

There are also some limitations and future directions in our study. First, activation of the p53 signaling pathway by knocking down VDR inhibits tumor oxidative stress was found in this study, but how does p53 inhibit oxidative stress in ESCC should to be further explored. Second, we found the activation of the LXR/RXR signaling pathway after VDR knockdown also inhibited the oxidative stress of ESCC, however, in-depth study is warranted to make it clear what the marker genes of LXR/RXR signaling pathway are associated to VDR's expression change. Third, more samples of clinic tissues are needed to validate our findings.

In summary, we demonstrated that VDR acts as a tumor-promotive factor in the progression of human ESCC, and VDR knockdown inhibits tumorigenesis. VDR participates in regulating TP53-suppressed ESCC cell oxidative stress and induces cell proliferation, metastasis, and invasion. These results revealed the effect of VDR on ESCC progression, thereby, challenging the traditional that VDR combined with vitamin D has an antitumor effect. Furthermore, our findings provide new insight into the mechanisms of ESCC progression, as well as into the influence of oxidative stress on the malignant behavior of ESCC. Oxidative stress may be a potential method to screen out relevant target molecules and provide a reliable basis for the clinical diagnosis and treatment of ESCC.

Data availability

The data associated with our study has been deposited into a publicly available repository, here attaching the website of the repository for accession: https://www.jianguoyun.com/p/DczCcmAQ6pO5ChjAvsAEIAA.

Conflict of interest and funding disclosure

The authors declare that they have no known competing financial interests or personal relationships that could have appeared to influence the work reported in this paper.

Ethical statement

The authors are accountable for all aspects of the work in ensuring that questions related to the accuracy or integrity of any part of the work are appropriately investigated and resolved. The study was conducted in accordance with the Declaration of Helsinki (as revised in 2013), and was reviewed and approved by the human participants' committee of West China Hospital of Sichuan University (approval number: No. 2021762 A), and the approval from Animal Ethics Committee of West China Hospital of Sichuan University

(approval number: No:20,220,211,008) and all patients provided informed consent to participate in the study. The permission to use of resected specimens and thewritten consents were obtained preoperatively.

All experimental procedures were approved by the institutional and local committee on the care and use of animals of West China Hospital of Sichuan University (Chengdu, China), and all animals received human care according to the National Institutes of Health (USA) guidelines.

CRediT authorship contribution statement

Qi-Xin Shang: Writing – review & editing, Writing – original draft, Validation, Methodology, Data curation. **Yu-Shang Yang:** Visualization, Resources, Methodology, Conceptualization. **Han-Lu Zhang:** Writing – review & editing, Writing – original draft, Resources. **Ya-Ping Cheng:** Software, Investigation, Data curation. **Han Lu:** Writing – original draft, Data curation, Conceptualization. **Yong Yuan:** Methodology, Investigation. **Long-Qi Chen:** Validation, Supervision, Software, Formal analysis, Conceptualization. **Ai-Fang Ji:** Project administration, Funding acquisition, Formal analysis.

Declaration of competing interest

The authors declare that they have no known competing financial interests or personal relationships that could have appeared to influence the work reported in this paper.

Acknowledgments

This work was supported by the Post-Doctor Research Project, West China Hospital, Sichuan University (2021HXBH090); Sichuan University Postdoctoral Interdisciplinary Innovation Fund (JCXK2224); Service Industry Innovation Discipline Group Construction of Shanxi Province (Jin Education and Research [2018] No.4); Key medical research project of science and technology innovation plan of Shanxi Provincial Health Commission-Key research projects (Jin Wei Science and Education Letter 2020XM17 [2021] No.9); Medical Science and Technology Innovation Team of science and technology Innovation plan of Shanxi Provincial Health Commission (Jin Wei Science and Education Letter 2020TD1 [2021] No.9), and 1•3•5 project for disciplines of excellence–Clinical Research Incubation Project, West China Hospital, Sichuan University (2018HXFH020).

Abbreviations

APOE	Apolipoprotein E
95%CI	95 % Confidence Interval
DAB	3,3′-Diaminobenzidine
ESCC	Esophageal squamous cell carcinoma
FBS	Fetal Bovine Serum
HR	Hazard Ratio
HRP	Horseradish Peroxidase
IPKB	Ingenuity Pathway Knowledge Base
IPA	Ingenuity Pathway Analysis
KEGG	Kyoto Encyclopedia of Genes and Genomes
KOALA	KEGG Orthology And Links Annotation
NC	Negative Control
OR	Odds Ratio
PBS	Phosphate Buffer Saline
PCA	Principal Component Analysis
PRM	Parallel Reaction Monitoring
RT-qPCR	Reverse Transcription-quantitative Polymerase Chain Reaction
ROS	Reactive Oxygen Species
shRNA	short hairpin RNA
SNP	Single Nucleotide Polymorphism
RXR	Retinoid X Receptor
TCGA	The Cancer Genome Atlas
TMA	Tissue Microarray
TMT	Tandem Mass Tags
VDR	Vitamin D Receptor
VDRE	Vitamin D Response Element

Appendix A. Supplementary data

Supplementary data to this article can be found online at https://doi.org/10.1016/j.heliyon.2023.e23832.

References

[1] J. Ferlay, I. Soerjomataram, R. Dikshit, et al., Cancer incidence and mortality worldwide: sources, methods and major patterns in GLOBOCAN 2012, Int. J. Cancer 136 (5) (2015) E359–E386.
[2] A. Jemal, F. Bray, M.M. Center, et al., Global cancer statistics, Ca - Cancer J. Clin. 61 (2) (2011) 69–90.
[3] L. Ma, Y.J. Xu, J.Z. Yang, et al., The relationship between plasma vitamin D level and the occurrence of esophageal squamous cell carcinoma, Chin. J. Intern. Med. 54 (1) (2015) 50–51.
[4] J. Yang, H. Wang, A. Ji, et al., Vitamin D signaling pathways confer the susceptibility of esophageal squamous cell carcinoma in a northern Chinese population, Nutr. Cancer 69 (4) (2017) 593–600.
[5] S.A. Ingles, R.K. Ross, M.C. Yu, et al., Association of prostate cancer risk with genetic polymorphisms in vitamin D receptor and androgen receptor, J. Natl. Cancer Inst. 89 (2) (1997) 166–170.
[6] M.R. Haussler, D.J. Mangelsdorf, B.S. Komm, et al., Molecular biology of the vitamin D hormone, Recent Prog. Horm. Res. 44 (1988) 263–305.
[7] S.E. Taymans, S. Pack, E. Pak, et al., The human vitamin D receptor gene (VDR) is localized to region 12 cen-q12 by fluorescent in situ hybridization and radiation hybrid mapping: genetic and physical VDR map, J. Bone Miner. Res. 14 (7) (1999) 1163–1166.
[8] J.M. Zmuda, J.A. Cauley, R.E. Ferrell, Molecular epidemiology of vitamin D receptor gene variants, Epidemiol. Rev. 22 (2) (2000) 203–217.
[9] L.A. Crofts, M.S. Hancock, N.A. Morrison, et al., Multiple promoters direct the tissue-specific expression of novel N-terminal variant human vitamin D receptor gene transcripts, Proc. Natl. Acad. Sci. U. S. A. 95 (18) (1998) 10529–10534.
[10] V. Rai, J. Abdo, S. Agrawal, et al., Vitamin D receptor polymorphism and cancer: an update, Anticancer Res. 37 (8) (2017) 3991–4003.
[11] P. Lips, Vitamin D physiology, Prog. Biophys. Mol. Biol. 92 (1) (2006) 4–8.
[12] J.C. Fleet, M. DeSmet, R. Johnson, et al., Vitamin D and cancer: a review of molecular mechanisms, Biochem. J. 441 (1) (2012) 61–76.
[13] G. Picotto, A.C. Liaudat, L. Bohl, et al., Molecular aspects of vitamin D anticancer activity, Cancer Invest. 30 (8) (2012) 604–614.
[14] C.D. Davis, Vitamin D and cancer: current dilemmas and future research needs, Am. J. Clin. Nutr. 88 (2) (2008) 565S–569S.
[15] S.A. Lamprecht, M. Lipkin, Cellular mechanisms of calcium and vitamin D in the inhibition of colorectal carcinogenesis, Ann. N. Y. Acad. Sci. 952 (2001) 73–87.
[16] I. Chung, G. Han, M. Seshadri, et al., Role of vitamin D receptor in the antiproliferative effects of calcitriol in tumor-derived endothelial cells and tumor angiogenesis in vivo, Cancer Res. 69 (3) (2009) 967–975.
[17] J. Reichrath, L. Rafi, M. Rech, et al., Analysis of the vitamin D system in cutaneous squamous cell carcinomas, J. Cutan. Pathol. 31 (3) (2004) 224–231.
[18] C.M. Hansen, L. Binderup, K.J. Hamberg, et al., Vitamin D and cancer: effects of 1,25(OH)2D3 and its analogs on growth control and tumorigenesis, Front. Biosci. 6 (2001) D820–D848.
[19] J.E. Osborne, P.E. Hutchinson, Vitamin D and systemic cancer: is this relevant to malignant melanoma? Br. J. Dermatol. 147 (2) (2002) 197–213.
[20] S.A. Lamprecht, M. Lipkin, Chemoprevention of colon cancer by calcium, vitamin D and folate: molecular mechanisms, Nat. Rev. Cancer 3 (8) (2003) 601–614.
[21] J.A. Taylor, A. Hirvonen, M. Watson, et al., Association of prostate cancer with vitamin D receptor gene polymorphism, Cancer Res. 56 (18) (1996) 4108–4110.
[22] J.E. Curran, T. Vaughan, R.A. Lea, et al., Association of a vitamin D receptor polymorphism with sporadic breast cancer development, Int. J. Cancer 83 (6) (1999) 723–726.
[23] C. Rouphael, A. Kamal, M.R. Sanaka, et al., Vitamin D in esophageal cancer: is there a role for chemoprevention? World J. Gastrointest. Oncol. 1 (2018) 23–30, 10.
[24] X. Wu, W. Hu, L. Lu, et al., Repurposing vitamin D for treatment of human malignancies viatargeting tumor microenvironment, Acta Pharm. Sin. B 9 (2) (2019) 203–219.
[25] Z. Zhou, Y. Xia, S. Bandla, et al., Vitamin D receptor is highly expressed in precancerous lesions and esophageal adenocarcinoma with significant sex difference, Hum. Pathol. 45 (8) (2014) 1744–1751.
[26] Y. Bao, S. Zhang, Y. Guo, et al., Stromal expression of JNK1 and VDR is associated with the prognosis of esophageal squamous cell carcinoma, Clin. Transl. Oncol. 20 (9) (2018) 1185–1195.
[27] M.G. Thomas, S. Tebbutt, R.C. Williamson, Vitamin D and its metabolites inhibit cell proliferation in human rectal mucosa and a colon cancer cell line, Gut 33 (12) (1992) 1660–1663.
[28] B.A. Laffitte, J.J. Repa, S.B. Joseph, et al., LXRs control lipid-inducible expression of the apolipoprotein E gene in macrophages and adipocytes, Proc. Natl. Acad. Sci. U. S. A. 98 (2) (2001) 507–512.
[29] J.R. Wiśniewski, A. Zougman, N. Nagaraj, et al., Universal sample preparation method for proteome analysis, Nat. Methods 6 (5) (2009) 359–362.
[30] M. Kanehisa, Y. Sato, K. Morishima, BlastKOALA and GhostKOALA: KEGG tools for functional characterization of genome and metagenome sequences, J. Mol. Biol. 428 (4) (2016) 726–731.
[31] P. Horton, K.J. Park, T. Obayashi, et al., WoLF PSORT: protein localization predictor, Nucleic Acids Res. 35 (2007) W585–W587. Web Server issue.
[32] J. Reichrath, S. Reichrath, K. Heyne, et al., Tumor suppression in skin and other tissues via cross-talk between vitamin D- and p53-signaling, Front. Physiol. 5 (2014) 166.
[33] R. Kommagani, V. Payal, M.P. Kadakia, Differential regulation of vitamin D receptor (VDR) by the p53 Family: p73-dependent induction of VDR upon DNA damage, J. Biol. Chem. 41 (2007) 29847–29854, 282.
[34] R. Maruyama, F. Aoki, M. Toyota, et al., Comparative genome analysis identifies the vitamin D receptor gene as a direct target of p53-mediated transcriptional activation, Cancer Res. 66 (9) (2006) 4574–4583.
[35] K.K. Deeb, D.L. Trump, C.S. Johnson, Vitamin D signalling pathways in cancer: potential for anticancer therapeutics, Nat. Rev. Cancer 7 (9) (2007) 684–700.
[36] F. Silvagno, C.B. Poma, C. Realmuto, et al., Analysis of vitamin D receptor expression and clinical correlations in patients with ovarian cancer, Gynecol. Oncol. 119 (1) (2010) 121–124.
[37] D. Matusiak, G. Murillo, R.E. Carroll, et al., Expression of vitamin D receptor and 25-hydroxyvitamin D3-1{alpha}-hydroxylase in normal and malignant human colon, Cancer Epidemiol. Biomarkers Prev. 14 (10) (2005) 2370–2376.
[38] D. Salehin, C. Haugk, M. Thill, et al., Vitamin D receptor expression in patients with vulvar cancer, Anticancer Res. 32 (1) (2012) 283–289.
[39] P.E. Hutchinson, J.A. Halsall, S. Popovici, et al., Compromised vitamin D receptor signalling in malignant melanoma is associated with tumour progression and mitogen-activated protein kinase activity, Melanoma Res. 28 (5) (2018) 410–422.
[40] B. Czogalla, E. Deuster, Y. Liao, et al., Cytoplasmic VDR expression as an independent risk factor for ovarian cancer, Histochem. Cell Biol. 154 (4) (2020) 421–429.
[41] K. Wada, H. Tanaka, K. Maeda, et al., Vitamin D receptor expression is associated with colon cancer in ulcerative colitis, Oncol. Rep. 22 (5) (2009) 1021–1025.
[42] R. Trowbridge, S.K. Mittal, P. Sharma, et al., Vitamin D receptor expression in the mucosal tissue at the gastroesophageal junction, Exp. Mol. Pathol. 93 (2) (2012) 246–249.
[43] S. McCain, J. Trainor, D.T. McManus, et al., Vitamin D receptor as a marker of prognosis in oesophageal adenocarcinoma: a prospective cohort study, Oncotarget 9 (2018) 34347–34356, 76.
[44] H.D. Qin, X.Y. Liao, Y.B. Chen, et al., Genomic characterization of esophageal squamous cell carcinoma reveals critical genes underlying tumorigenesis and poor prognosis, Am. J. Hum. Genet. 98 (4) (2016) 709–727.
[45] J. Sun, X. Fu, Y. Wang, et al., Erianin inhibits the proliferation of T47D cells by inhibiting cell cycles, inducing apoptosis and suppressing migration, Am. J. Transl. Res. 8 (7) (2016) 3077–3086.
[46] A.J. Levine, M. Oren, The first 30 years of p53: growing ever more complex, Nat. Rev. Cancer 10 (2009) 749–758, 9.
[47] Z. Wang, C. Li, Y. Li, et al., DpdtbA-induced growth inhibition in human esophageal cancer cells involved inactivation of the p53/EGFR/AKT pathway, Oxid. Med. Cell. Longev. 2019 (2019), 5414670.
[48] N. Melling, S. Norrenbrock, M. Kluth, et al., p53 overexpression is a prognosticator of poor outcome in esophageal cancer, Oncol. Lett. 17 (4) (2019) 3826–3834.

[49] F. Attaran-Bandarabadi, A.A. Ziaee, M. Yazdanbod, et al., Loss of heterozygosity on chromosome 5 in Iranian esophageal cancer patients, Genet. Mol. Res. 10 (4) (2011) 2316–2351.
[50] C. Hong, P. Tontonoz, Liver X receptors in lipid metabolism: opportunities for drug discovery, Nat. Rev. Drug Discov. 13 (6) (2014) 433–444.
[51] F. Bovenga, C. Sabbà, A. Moschetta, Uncoupling nuclear receptor LXR and cholesterol metabolism in cancer, Cell Metabol. 4 (2015) 517, 21.
[52] I. Dalle-Donne, R. Rossi, R. Colombo, et al., Biomarkers of oxidative damage in human disease, Clin. Chem. 52 (4) (2006) 601–623.
[53] A. Agarwal, A. Aponte-Mellado, B.J. Premkumar, et al., The effects of oxidative stress on female reproduction: a review, Reprod. Biol. Endocrinol. 10 (2012) 49.
[54] S. Tangvarasittichai, Oxidative stress, insulin resistance, dyslipidemia and type 2 diabetes mellitus, World J. Diabetes 6 (3) (2015) 456–480.
[55] E.S. Hwang, P.E. Bowen, DNA damage, a biomarker of carcinogenesis: its measurement and modulation by diet and environment, Crit. Rev. Food Sci. Nutr. 47 (1) (2007) 27–50.
[56] K. Ishikawa, K. Takenaga, M. Akimoto, et al., ROS-generating mitochondrial DNA mutations can regulate tumor cell metastasis, Science 320 (2008) 661–664, 5876.
[57] E. Gottlieb, I.P. Tomlinson, Mitochondrial tumour suppressors: a genetic and biochemical update, Nat. Rev. Cancer 11 (2005) 857–866, 5.
[58] K. Beyfuss, D.A. Hood, A systematic review of p53 regulation of oxidative stress in skeletal muscle, Redox Rep. 23 (1) (2018) 100–117.